JOURNAL OF Applied Polymer SCIENCE

Characterization and Anticorrosive Properties of Poly(2,3-dimethylaniline)/Na^+-Montmorillonite Composite Prepared by Emulsion Polymerization

Li Ma, Dan-Dan Fu, Meng-Yu Gan, Feng Zhang, Zhi-Tao Li, Sha Li
College of Chemistry and Chemistry Engineering, Chongqing University, Chongqing City 400030, People's Republic of China
Correspondence to: L. Ma (E-mail: mlsys607@126.com)

ABSTRACT: Composites of Poly(2,3-dimethylaniline) and inorganic Na^+-montmorillonite clay were synthesized by emulsion polymerization. The as-synthesized composites (PDMA) were characterized by Fourier Transform Infrared Spectroscopy, X-ray diffraction, and scanning electron microscopy. The protective performance against corrosion of the samples was evaluated by Tafel and electrochemical impedance spectroscopy measurements. The results showed that the composite containing 5 wt. % of clay loading (PDMA-5%) displayed a better anticorrosive performance than other samples. The Epoxy(E) blend with PDMA-5% (EPM5) coating was founded to have a higher corrosion potential and a lower current density than that of Epoxy blend P(2,3-DMA) (EP) coating. The impedance value of EPM5 coating was about $6.68\times10^6\Omega\cdot cm^2$ in 5 wt. % NaCl solution even after 288 h, compared to EP ($4.26\times10^5\Omega\cdot cm^2$) coating, which went to show that the corrosion inhibition of P(2,3-DMA) could be effectively enhanced by incorporating MMT into the P(2,3-DMA) matrix. © 2013 Wiley Periodicals, Inc. J. Appl. Polym. Sci. 130: 4528–4533, 2013

KEYWORDS: poly(2,3-dimethylaniline) clay; corrosion; emulsion polymerization; composite

Received 9 October 2012; accepted 28 March 2013; Published online 27 July 2013
DOI: 10.1002/app.39364

INTRODUCTION

Recently, polyaniline (PANI) has become a good candidate in anticorrosion coating to replace chromium-containing materials, which have adverse effect on health and environment.[1–6] However, PANI has always been considered as an intractable material because of its poor solubility in most organic solvents, with a result of limiting its further practical application. Therefore, several approaches have been explored, including alkyl, alkoxy, and amino ring-substituted[7–10] and *N*-substituted[11,12] PANI derivatives, which have attracted widely attention owing to their relatively good solubility in common solvents. 2, 3-dimethylaniline (2,3-DMA) as an aniline derivative has two electron-donating methylic substituent in the benzene ring. Many researches indicated that electron-donating groups can lead to a larger steric volume among molecular chains, which can contribute to the increase of solubility and corrosion performance.[13] The corrosion property of P(2,3-DMA) was also reported by Ma et al.[14] who confirmed that the anticorrosive performance of the polymer P(2,3-DMA) is better than the parent polymer PANI.

In general, the primary effects of polymeric coatings are to function as physical barrier against aggressive species such as O_2 and H^+. However, not all polymeric coatings are permanently impenetrable, and once there are defects in the coatings, pathways will be formed for the corrosive species to attack the metallic substrate and localized corrosion will occur.[15] Therefore, montmorillonite (MMT) as a layered material, whose lattice is composed of an edge-shared octahedral alumina sheet sandwiched between two tetrahedral silica sheets, and the lamellar elements of MMT such as aluminum flakes can be introduced into the polymeric coating to effectively increase the length of the diffusion pathways for oxygen and water as well as decrease the permeability of the coating.[16,17] Based on the reports of published literature, the corrosion resistance of pristine polymer e.g. PANI,[18,19] polystyrene,[20] poly(methyl methacrylate),[21,22] polysulfone[23] can be effectively enhanced by incorporating inorganic nanolayers of MMT clay into polymeric matrix. So, it is necessary to combine the advantages of these polymers and MMT to obtain better corrosion protection for common metals.

In this article, the incorporation of MMT into P(2,3-DMA) matrix was prepared by emulsion polymerization to enhance the corrosion protection of P(2,3-DMA). The as-prepared materials were characterized by X-ray diffraction (XRD), Fourier Transform Infrared Spectroscopy (FTIR), and scanning electron microscope (SEM), and the anticorrosive performance of the coatings containing P(2,3-DMA) and PDMA on iron samples was evaluated by electrochemical measurements in 5 wt % NaCl solution.

© 2013 Wiley Periodicals, Inc..

EXPERIMENTAL

Materials and Instruments

2,3-dimethylaniline monomer (2,3-DMA) was obtained from Besmet company, Zhejiang. Dodecylbenzene sulfonic acid (DBSA, Chongqing) and ammonium peroxydisulfate (APS, Chongqing) were used as surfactant and oxidant, respectively. Sodium montmorillonite (Na^+-MMT) with a cation exchange capacity of 100 meq/100 g was purchased from FengHong Company, Zhejiang. All other reagents were analytical grade and used as received.

XRD patterns were tested on a D/Max2500 VBI+/PC diffractometer with Cμ-Kα radiation at 40 kV and 50 mA. FTIR of the samples in KBr pellets were recorded on a Nicolet550 II FTIR spectrometer ranging from 500 to 4000 cm^{-1}. The morphology of the composite was examined by Scanning electron microscope (SEM, FEI NOVA 400 NANO). The electrochemical studies were carried out with CHI660 electrochemical analyzer with the loaded carbon paper[24,25] as working electrode, the saturated calomel electrode used as the reference electrode,and a platinum sheet was used as counter electrode. Polarization curve was carried out in the potential window ranging from −0.4 to 0.4 V at a scan rate of 10 mV/s. Electrochemical impedance spectroscopy (EIS) was characterized at open circuit potential in the frequency range from 10^5 to 10^{-2} Hz.

Preparation of P(2,3-DMA)/MMT and Carbon Paper Loaded Electrode

The powder forms of the PDMA composites were synthesized through the emulsion polymerization.[26,27] The desired amount of Na^+-MMT was prepared in an aqueous medium and then vigorously stirred overnight for swelling of the Na^+-MMT, followed by adding suitable amount of 1.0*M* HCl aqueous solution to adjust the pH to about 3-4. 0.05 mol DBSA, 0.016 mol 2,3-dimethylaniline, and 100 mL distilled water were successively added to a three-necked flask. The solution was stirred to form uniformly dispersed 2,3-dimethylaniline-DBSA emulsion. After that, the emulsion was added into the previously clay solution under magnetically stirring for 2 h. Then pieces of carbon paper were put into the mixed solution with stirring for 30 min. Subsequently, 0.024 mol of APS dissolving in 25 mL distilled water was added into the prepared solution under a constant stirring by dropwise. The samples were polymerized in a water bath at 30°C for 12 h.

The above obtained emulsion was demulsified by adding excess acetone under magnetically stirring for 0.5 h and the PDMA powder was obtained by washing, filtering, drying, and milling, sequentially. At the same time, the loaded PDMA carbon paper was taken out as the working electrode for subsequent use to study the effect of clay on the corrosion protection of PDMA. The P(2,3-DMA)-DBSA materials without clay were synthesized by the same emulsion polymerization.

Preparation of Coatings and Electrochemical Measurements

For preparation of the coatings, 2 g P(2,3-DMA)-5%MMT (PDMA-5%) powder was suspended in 30 mL acetic ether, and then 48 g Epoxy(E) resin dissolving in 20 mL Xylene was mixed with the above suspension. The mixture was stirred by the magnetic stirrer for about 8 h. After vigorous stirring, the homogeneous composite was achieved. The liquid paint was coated on iron samples and then samples were dried at 60°C for 24 h. The coating-coated iron samples were used as the working electrode to study the anticorrosive performance of PDMA/Epoxy (EPM) coating. For comparison, P(2,3-DMA)/Epoxy (EP) coated samples were also prepared.

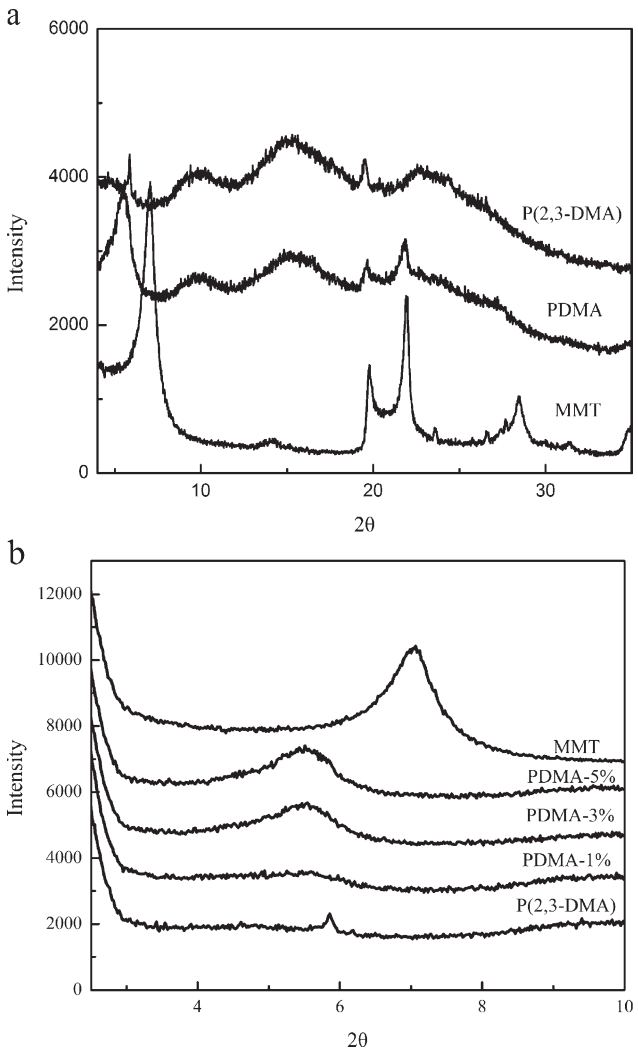

Figure 1. Comparison of X-ray diffraction patterns of (a) the MMT clay, P (2, 3-DMA), and P (2, 3-DMA)/clay samples and of (b) PDMA samples with various MMT molar concentrations.

RESULTS AND DISCUSSION

Characterization

XRD patterns of MMT clay, P(2,3-DMA) and a series of PDMA composites were given in Figure 1. The peak of the clay at ≈7° shown in Figure 1(a) assigned to the periodicity in the (001) direction of MMT clay. The (001) peak was shifted to a lower angles for PDMA composites, indicating the intercalation of P(2,3-DMA) between the clay layers. Moreover, the d-spacing (d001) of interlayer of MMT was about 1.25 nm calculated by the Bragg's equation ($d = \lambda/2\sin\theta$), and that of PDMA-3% composite was about 1.59 nm in Figure1(b). This result demonstrated that the P(2,3-DMA)

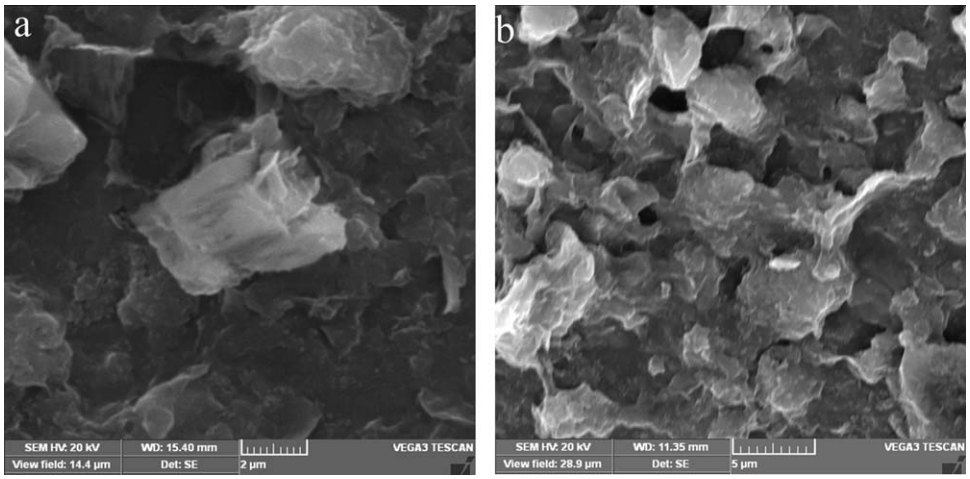

Figure 2. SEM images of (a) MMT and (b) PDMA composite.

chains were inserted into the interlayer of clay and expanded the interlayer spacing. For PDMA-5%, the further increase in interlayer distance of MMT was not observed, indicating that some of MMT clay cannot be exfoliated in the P(2,3-DMA) matrix and existed in an intercalated layer structure. As for the reason, it might be due to the micelles[28] of 2,3-DMA and DBSA molecules formed during the polymerization process existed in an aggregated bulkier form, so the intercalation process was not good enough.

Figure 2 shows the SEM images of MMT clay and PDMA composite. From the SEM micrographs, we can learn that the pristine MMT has a flaky texture reflecting its layered structure and the PDMA composite has a granular texture.[29,30] This confirms that P(2,3-DMA) coating is produced on the surface of MMT. The tactoids plates and granular regions like P(2,3-DMA) can be seen.

The FTIR spectra of MMT, P(2,3-DMA) and PDMA composites were shown in Figure 3. The characteristic vibration bands of P(2,3-DMA) were located at 1111, 1319, 1382, 1473, 1582, and 2849 cm^{-1}. The peak at 2849 cm^{-1} was due to the saturated alkyl C—H stretching vibration, and the peak at 1382 cm^{-1} was assigned to the —CH_3 characteristic absorption, these data show that there were methyl substituent existed in P(2,3-DMA) backbone. The band at 1582 cm^{-1} was assigned to the C=C stretching vibration of the quinoid ring, and the peak at 1473 cm^{-1} was associated with the C=C stretching vibration of the benzenoid ring. The peak at 1319 cm^{-1} was attributed to the C—N stretching vibrations of quinoid ring, and the absorption peak at 1111 cm^{-1} was the characteristic of the C—H in-plane bending vibration.[14,31] The characteristic bands of MMT clay were presented at 1040 cm^{-1} (Si—O—Si), 520 cm^{-1} (Al—O) and 466 cm^{-1} (Mg—O). Therefore, the FT-IR spectra confirms the incorporation of MMT clay in P(2,3-DMA) matrix using emulsion polymerization.[32,33]

Effect of Clay on the Corrosion Protection of P(2,3-DMA)/MMT

The effect of clay on the corrosion protection of PDMA composites was performed in 3.5% NaCl solution using samples-loaded carbon paper as working electrode. Tafel (TAF) plots for (a) unloaded, (b) P(2,3-DMA)-loaded, (c) PDMA-1%-loaded, (d) PDMA-3%-loaded, (e) PDMA-5%-loaded, and (f) PDMA-7%-loaded carbon paper electrodes were shown in Figure 4. It should be noted that the E_{corr} values of P(2,3-DMA) and P(2,3-DMA)/MMT materials loaded carbon paper were more positive than that of unloaded electrode. Moreover, with the increasing loading of MMT clay in the P(2,3-DMA) matrix, the E_{corr} values of PDMA-1%, PDMA-3%, PDMA-5%, PDMA-7% were found to shift to a more positive direction of potential, reach maximum, and then decrease. The reason is that the excessive MMT clay loading may not be well intercalated in the P(2,3-DMA) matrix, but mixed up in PDMA composite. This could have a negative effect on the hindrance of electric and charge transfer, which may decrease the anticorrosive property of PDMA. When the incorporation of MMT clay loading is 5 wt %, the anticorrosion property is the best.

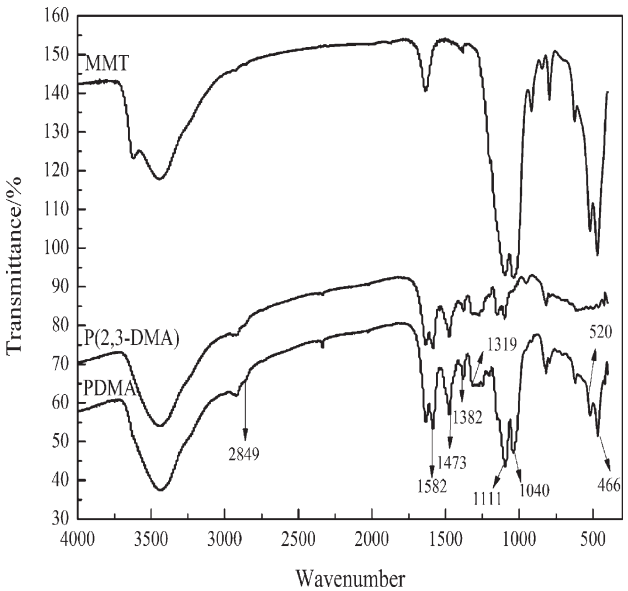

Figure 3. Comparison of FTIR spectra of MMT clay, P (2, 3-DMA) and PDMA samples.

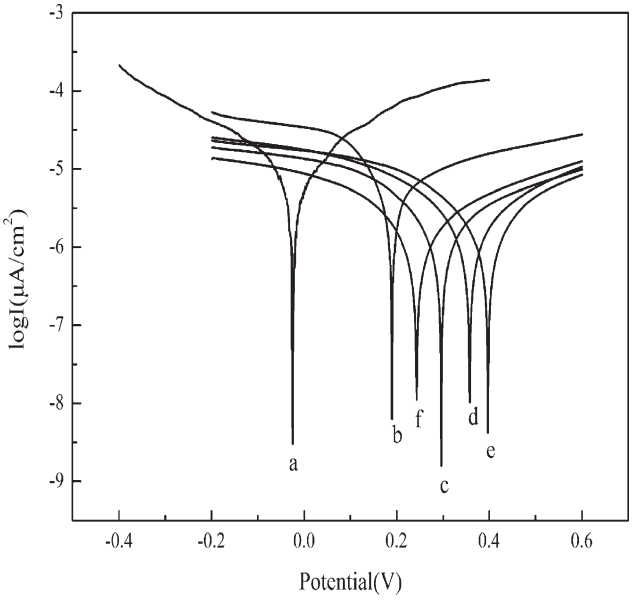

Figure 4. Tafel plots for (a) unloaded, (b) P(2,3-DMA)-loaded, (c) PDMA-1%-loaded, (d) PDMA-3%-loaded, (e) PDMA-5%, (f) PDMA-7%-loaded carbon paper, measured in 3.5% NaCl solution.

Figure 5 shows the Nyquist plots of the unloaded, P(2,3-DMA) loaded and a series of PDMA loaded carbon paper respectively. The charge-transfer resistances of the six samples, as determined by the intersection of the low-frequency end of the semicircle arc with the real axis, were 7168.1, 30421, 42148, 55290, 101000, 44173Ωcm^2, respectively. The results indicated that the incorporation of 5 wt. % of clay loading into P(2,3-DMA) matrix revealed a relatively better anticorrosive performance. This enhanced corrosion protection of PDMA compared to pure P(2,3-DMA) might result from the silicate nanolayers of clay

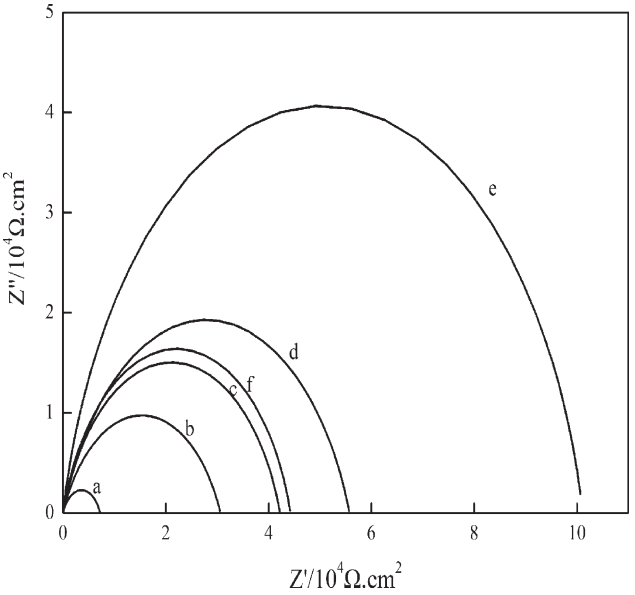

Figure 5. EIS for (a) unloaded, (b) P(2,3-DMA)-loaded, (c) PDMA-1%-loaded, (d) PDMA-3%-loaded, (e) PDMA-5%-loaded, (f) PDMA-7%-loaded carbon paper, measured in 3.5% NaCl solution.

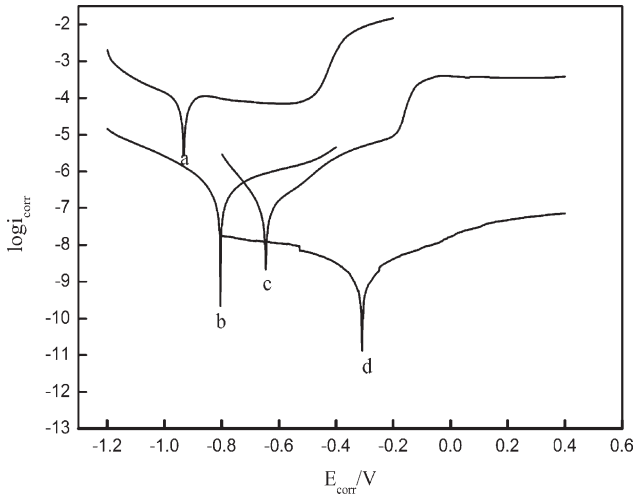

Figure 6. Tafel plots for (a) uncoated, (b) E-coated, (c) EP-coated, and (d) EPM5-coated iron samples.

dispersed in P(2,3-DMA) matrix which increase the tortuosity of diffusion pathway of corrosive agents such as oxygen gas, hydrogen, hydroxide ions.

Anticorrosion Performance of P(2,3-DMA)-MMT/Epoxy (EPM) Coating

Figure 6 shows the TAF plots for uncoated, Epoxy (E)-coated, P(2,3-DMA)/E (EP)-coated and PDMA-5%/E (EPM5)-coated steel electrodes, respectively. Furthermore, the anticorrosive performance of coatings is evaluated from the values of corrosion potential (E_{corr}), corrosion current (I_{corr}) and polarization (R_p), [28] as listed in Table I. The EP coating presented higher values in E_{corr} (−646 mV), R_p (1.56×10^3 KΩ·cm^2), and lower values in I_{corr} (1.01×10^{-3} A·cm^2) than the E coating ($E_{corr} = -804$ mV, $R_p = 2.84 \times 10^2$ KΩ·cm^2, and $I_{corr} = 3.24 \times 10^{-3}$ A·cm^2). This enhanced corrosion protection of EP coating compared to E coating resulted from the effect of a polymeric coating acting as a physical barrier against aggressive species. Moreover, the EPM5 coating has a higher corrosion potential (308 mV). The polarization resistance (R_p) value of EPM5 coating is about 2.90×10^3 K Ω·cm^2, which is about three orders of magnitude greater than the E coating. Therefore, the TAF curves indicate that the incorporation of clay into P(2,3-DMA) matrix can lead to a greatly increase of corrosion inhibition.

The appearance of the samples after salt spray test for 30 days is shown in Figure 7. It can be seen that the E-coated iron sample suffered from aggravating corrosion in large-scale with rust and

Table I. E_{corr}, I_{corr}, R_p for (a) Uncoated, (b) E-coated, (c) EP-coated, and (d) EPM5-Coated Iron Samples

	Electrochemical corrosion measurements		
Samples	E_{corr} (V)	I_{corr} (A·cm^2)	R_p (KΩ·cm^2)
Uncoated	−0.932	5.08×10^{-2}	7.74
E	−0.804	3.24×10^{-3}	2.84×10^2
EP	−0.646	1.01×10^{-3}	1.56×10^3
EPM5	−0.308	2.92×10^{-4}	2.90×10^3

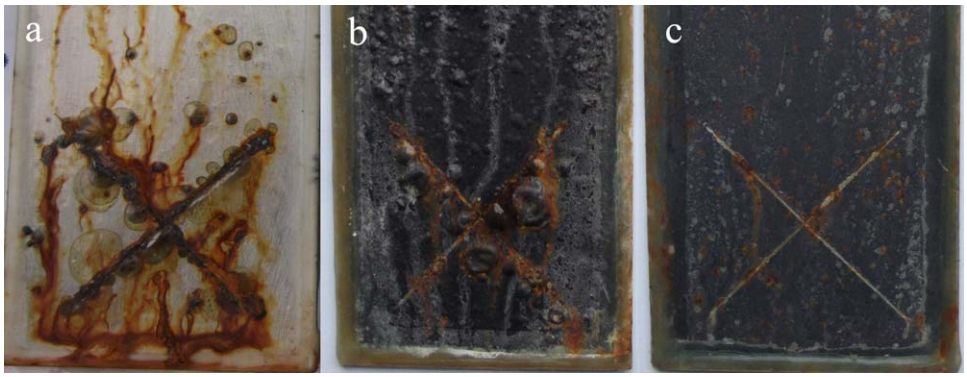

Figure 7. Photograph of (a) pure epoxy-coated steel, (b) EP-coated iron sample, and (c) EPM5-coated iron sample after 30 days of exposure to salt spray test. [Color figure can be viewed in the online issue, which is available at wileyonlinelibrary.com.]

blister, and the EP coating has more corrosion extended area from the scribes. Whereas localized corrosion was observed for EPM5 coating and a slight rust formation was found in the scribed areas. The result was consistent with the above observation made in electrochemical tests.

The bode plots of EPM5-coated and EP-coated steel in various immersion time in 5% NaCl solution are shown in Figure 8. The impedance value of EPM5 coating was founded to be greater than EP coating. The resistance value of EPM5 ($4.84 \times 10^6 \Omega \cdot cm^2$) coating after 10 days immersion was about 30 times compared to the EP ($1.45 \times 10^4 \Omega \cdot cm^2$) coating. Figure 9 shows the Nyquist plots of EPM5 in various immersion times. It can be seen that the charge transfer resistance value of EPM5 ($R_c = 6.68 \times 10^6 \Omega \cdot cm^2$) coating in long-time immersion time (288 h) was about 15 times with respect to the EP ($4.26 \times 10^5 \Omega \cdot cm^2$) coating. The enhanced corrosion protection of PDMA compared to pure P(2,3-DMA) associated with both the physical barrier effect of P(2,3-DMA) resulted from the larger steric volume among P(2,3-DMA) molecular chains and the silicate nanolayers of clay dispersed in P(2,3-DMA) matrix.

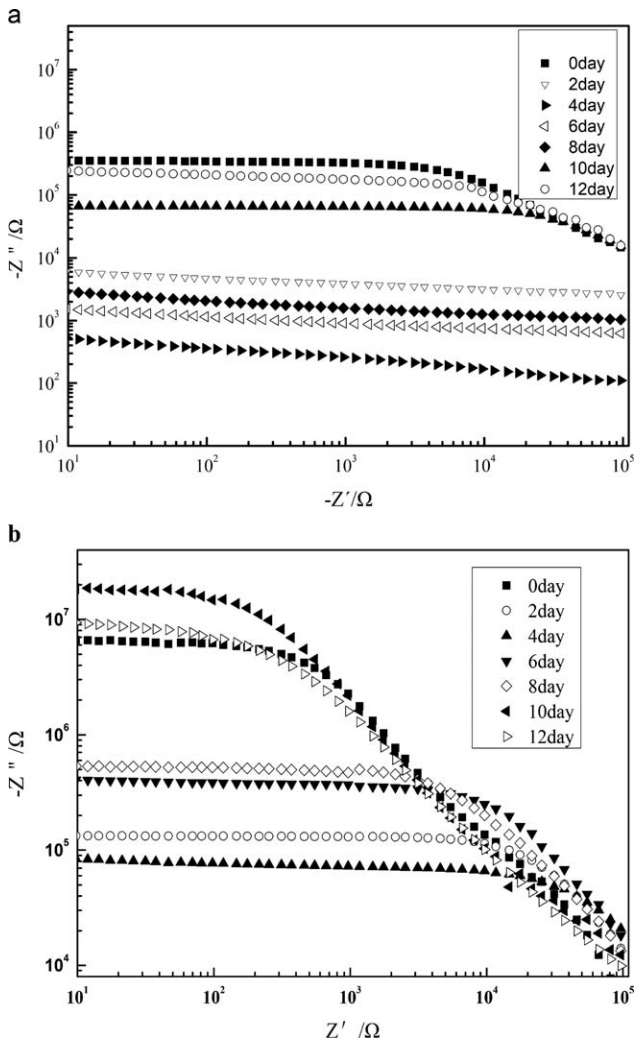

Figure 8. Bode plots of (a) EP-coated and (b) EPM5-coated iron samples in various immersion times in 5% NaCl solution.

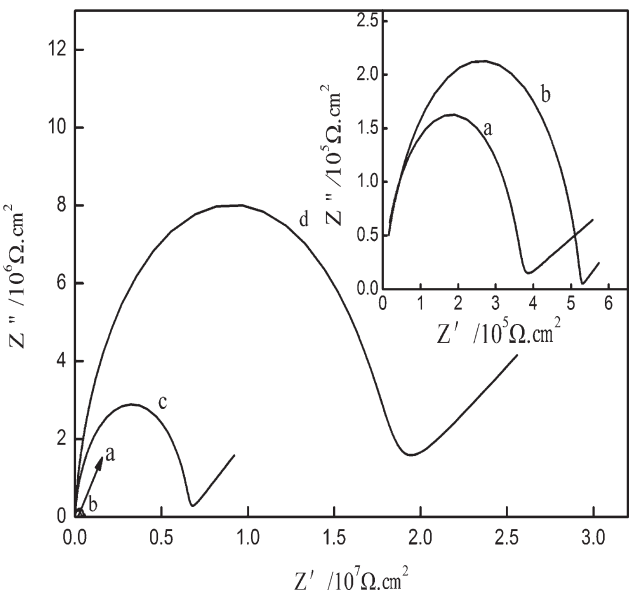

Figure 9. Nyquist plots of impedance spectra of EPM5-coated iron samples after (a) 6 days; (b) 8 days; (c) 10 days; (d) 12 days of immersion in 5% NaCl solution.

CONCLUSION

The composite of P(2,3-DMA) with MMT clay were synthesized by emulsion polymerization. The XRD and SEM results proved that P(2,3-DMA) chains have been inserted in the clay layers and an intercalated P(2,3-DMA)/MMT composite has been synthesized. The effect of clay on the corrosion protection of P(2,3-DMA)/MMT composite was performed by TAF and EIS measurements. PDMA-5%-loaded carbon paper electrode was found to be superior in anticorrosion over other samples in 3.5%NaCl electrolyte. The enhanced corrosion protection of EP coating relative to E coating was associated with the physical barrier of P(2,3-DMA) resulted from the larger steric volume among P(2,3-DMA) molecular chains. The anticorrosive performance of EPM5 coating on steel was founded to be better than pure EP coating in a long-time immersions time (288 h), and it resulted from the barrier effect of nanolayers of MMT dispersed in composites to increase the tortousity of diffusion pathway of water and oxygen molecules.

REFERENCES

1. Deberry, D. W. *J. Electrochem. Soc.* **1985**, *132*, 1027.
2. Wessling, B. *Synth. Met.* **1991**, *907*, 1057.
3. Soares, B. G.; Leyva, M. E.; Barra, G. M. O.; Khastgir, D. *Eur. Polym. J.* **2006**, *42*, 676.
4. Wrobleski, D. A.; Benicewicz, B. C.; Thompson, K. G.; Byran, C. *J. Polym. Prepr.* **1994**, *35*, 265.
5. Wessling, B. *Adv. Mater.* **1994**, *6*, 226.
6. Wei, Y.; Wang, J.; Jia, X.; Yeh, J.-M.; Spellane, P. *Polymer* **1995**, *36*, 4535.
7. Li, X. G.; Huang, M. R.; Duan, W.; Yang, Y. L. *Chem. Rev.* **2002**, *102*, 2925.
8. Savithaa, P.; Sathyanarayana, D. N. *Synth. Met.* **2003**, *145*, 113.
9. Savitha, P.; Sathyanarayana, D. N. *Polym. Int.* **2004**, *53*, 106.
10. Santhosh, P.; Sankarasubramanian, M.; Thanneermalai, M.; Gopalan, A.; Vasudevan, T. *Mater. Chem. Phys.* **2004**, *85*, 316.
11. Umare, S. S.; Borkar, A. D.; Gupta, M. C. *Bull. Mater. Sci.* **2002**, *25*, 235.
12. Bergeron, J. Y.; Dao, L. H. *Macromolecules* **1992**, *25*, 3332.
13. Sathiyanarayanan, S.; Balakrishnan, K.; Dhawan, S. K.; Trivedi, D. C. *Electrochim. Acta* **1994**, *39*, 831.
14. Ma, L.; Huang, C. Q.; Gan, M. Y. *J. Appl. Polym. Sci.* **2013**, *127*, 3699.
15. Yeh, J. M.; Liou, S. J.; Lin, C. Y.; Cheng, C. Y.; Chang, Y. W.; Lee, K. R. *Chem. Mater.* **2002**, *14*, 154.
16. Li, P.; Tan, T. C.; Lee, J. Y. *Synth. Met.* **1997**, *88*, 237.
17. Yeh, J. M.; Yao, C. T.; Hsieh, C. F.; Lin, L. H.; Chen, P. L.; Wu, J. C.; Yang, H. C.; Wu, C. P. *Eur. Polym. J.* **2008**, *44*, 3046.
18. Yeh, J.-M.; Liou, S.-J.; Lai, C.-Y.; Wu, P.-C.; Tsai, C.-Y. *Chem. Mater.* **2001**, *13*, 1131.
19. Yeh, J.-M.; Chen, C.-L.; Chen, Y.-C.; Ma, C.-Y.; Lee, K.-R.; Wei, Y.; Li, S. *Polymer* **2002**, *43*, 2729.
20. Yeh, J.-M.; Liou, S.-J.; Lin, C.-G.; Chang, Y.-P.; Yu, Y.-H. *J. Appl. Polym. Sci.* **2004**, *92*, 1970.
21. Yeh, J.-M.; Liou, S.-J.; Lin, C.-Y.; Cheng, C.-Y.; Chang, Y.-W.; Lee, K.-R. *Chem. Mater.* **2002**, *14*, 154.
22. Yeh, J.-M.; Liou, S.-J.; Lai, M.-C.; Chang, Y.-W.; Huang, C.-Y.; Chen, C.-P.; Jaw, J.-H.; Tsai, T.-Y.; Yu, Y.-H. *J. Appl. Polym. Sci.* **2004**, *94*, 1936.
23. Yeh, J.-M.; Chen, C.-L.; Chen, Y.-C.; Ma, C.-Y.; Yu, Y.-H.; Huang, H.-Y. *J. Appl. Polym. Sci.* **2004**, *92*, 631.
24. Ma, L.; Luo, L. Z.; Gan, M. Y.; Li, X. F.; Su, W. Y.; Yan, J.; Tang, J. H. *Acta Chim. Sin.* **2010**, *68*, 814.
25. Ma, L.'; Luo, L. Z.; Ma, H. T.; Li, X. F.; Su, W. Y.; Hao, S. N. *Chin. J. Chem.* **2010**, *28*, 1871.
26. Yeh, J. M.; Kuo, T. H.; Huang, H. J.; Chang, K. C.; Chang, M. Y.; Yang, J. C. *Eur. Polym. J.* **2007**, *43*, 1624.
27. Chang, K. C.; Lai, M. C.; Peng, C. W.; Chen, Y. T.; Yeh, M. J.; Lin, C. L. *Acta Mater.* **2006**, *51*, 5645.
28. (a) Sapurina, I.; Stejskal, J.; Tuzar, Z. *Colloids Surf. A.* **2001**, *180*, 193; (b) Noriyuki, K..; Genies, E. M. *Synth. Met.* **1995**, *68*, 191.
29. Wan, M.; Li, M.; Li, J.; Liu, Z. *J. Appl. Polym. Sci.* **1994**, *53*, 131.
30. Sivakumar, S.; Damodaran, A. D.; Warrier, K. G. K. *Ceram. Int.* **1995**, *21*, 85.
31. Gu, J.; Ma, L.; Gan. M.; Zhang, F.; Li, W.; Huang, C. *Thermochim. Acta* **2012**, *549*, 13.
32. Chang, K. C.; Chen, S. T.; Lin, H. F.; Lin, C. Y.; Huang, H. H.; Yeh, J. M.; Yu, H. Y. *Eur. Polym. J.* **2008**, *44*, 13–23.
33. Yu, Y. H.; Yeh, J. M.; Liou, S. J.; Chen, C. L.; Liaw, D. J.; Lu, H. Y. *J. Appl. Polym. Sci.* **2004**, *92*, 3573.